

Detection of gravitational wave bursts by interferometric detectors

Nicolas Arnaud,* Fabien Cavalier, Michel Davier, and Patrice Hello

Laboratoire de l'Accélérateur Linéaire, B.P. 34, Bâtiment 200, Campus d'Orsay, 91898 Orsay Cedex, France

(Received 8 October 1998; published 9 March 1999)

We study some filters for the detection of burstlike signals in the data of interferometric gravitational wave detectors. We present first two general (nonlinear) filters with no *a priori* assumption on the waveforms to detect. A third filter, a peak correlator, is also introduced and permits us to estimate the gain, when some prior information is known about the waveforms. We use the catalog of supernova gravitational wave signals built by Zwerger and Müller in order to have a benchmark of the performance of each filter and to compare to the performance of the optimal filter. The three filters could be a part of an on-line triggering in interferometric gravitational wave detectors, specialized in the selection of burst events. [S0556-2821(99)01706-3]

PACS number(s): 04.80.Nn, 07.05.Kf

I. INTRODUCTION

Long-base-line interferometric gravitational-wave detectors such as The Laser Interferometric Gravitational Wave Observatory (LIGO) [1], VIRGO [2], GEO600 [3], or TAMA300 [4] are now in their phase of construction, and should be fully operational in the first years of the next millennium. Sources of gravitational waves that are expected in the bandwidth of these detectors all involve compact objects such as black holes (BHs) or neutron stars (NSs); see [5] or [6] for a review. Among them, inspiraling binaries seem to be the most promising sources for a first direct detection of gravitational waves. Accordingly, a huge effort has been made up to now in order to be ready in time for analyzing the inspiraling binary data delivered by the interferometric detectors: detection of the signal by correlation with suitable templates (matched filtering) (see, e.g., [7–10]) or by time-frequency analysis [11,12] and estimation of astrophysical parameters (mainly the masses of the stars and their spins) [13–15]. This part of gravitational wave data analysis, concerning inspiraling compact binaries, is now well advanced and rather well understood. In addition, periodic sources such as rotating neutron stars are maybe as interesting as the binary inspirals, since, despite the low expected gravitational wave amplitudes, these sources have the advantage of being permanent. A number of studies have been also dedicated to the analysis of periodic sources: see, e.g., [7] or [16] and references therein.

Historically, supernovas (SNS) were the first envisaged gravitational wave emitters and first resonant detectors have been designed to be sensitive around the typical frequencies expected in such bursts of gravitational radiation, around 1 kHz. With the construction of intrinsically broadband interferometric detectors, these kinds of sources have not been studied as much as inspiraling binaries or pulsars.

Expected sources of burst gravitational waves are first collapses of massive stars to neutron stars (type II SNS) or to black holes. Modern simulations of the former show a rather small efficiency of gravitational radiation emission [17–21]:

amplitudes typically less than 10^{-22} are expected for SNS at the distance of the Virgo cluster. Nevertheless, observation of very fast pulsars in the Galaxy (such as the one in the Guitar Nebula [22]) may indicate that, at least in some cases, the collapse can be highly asymmetric and provides much higher gravitational wave strain amplitudes [23]. Estimates of gravitational wave amplitudes from the collapse to a BH reach similar orders of magnitude as for previous type II SNS [24,6].

Another possible source of gravitational wave bursts occurs during the merging of two compact stars, at the very end of the binary inspiral. If the inspiral signal for binary neutrons stars is well understood up to the 2.5 post-Newtonian order [25], we know only little about the signal waveform corresponding to the merging phase itself, since its computation requires in particular fully relativistic hydrodynamical codes, although some semiclassical attempts have already been performed; see, e.g., [26]. Some recent estimates [27] give a maximum amplitude $h \sim$ a few 10^{-21} at 10 Mpc within a frequency range of 1–2 kHz. This is just the order of magnitude of the noise level at these frequencies for interferometric detectors in their initial design; that leaves some hope for a future detection. Concerning BH binaries, an ambitious program called The Binary Black Hole Grand Challenge Alliance [28] is underway to handle the very difficult task of computing the waveform of the merging phase.

Damped oscillations of excited BHs or NSs, like baby born NSs (just after the collapse), can also provide gravitational waves with detectable amplitudes [6]. The corresponding waveforms are not really burst like; they rather have some coherent structure (they look like typically a damped sine). However, their characteristic frequencies, above hundreds of Hz to tens of kHz, and their short damping times make them belong to the category of signals of interest in this article. Note that the frequencies and damping times are exactly known for a Kerr BH [29] and the detection of gravitational waves emitted by such a perturbed BH could provide a direct measurement of both its mass and its angular momentum [30]; of course, in this case, matched filtering, with damped sine templates, is the more suitable method.

All these gravitational wave burst signals have the following features: short durations from milliseconds to seconds, frequencies from ~ 100 Hz to a few kHz, and a large range

*Also at Ecole Nationale des Ponts et Chaussées, 6-8 av. B. Pascal, Cité Descartes, 77455 Marne la Vallée, France.

of waveforms. Filtering of such short signals in the output of interferometric detectors should therefore be as general or robust as possible, and designed with (almost) no *a priori* knowledge of the waveforms; this prescription of course forbids the optimal (Wiener) filtering as used for inspiraling binaries. Such general filtering methods are then necessarily “suboptimal,” in the sense that they are less efficient than the optimal filtering. In this article, we concentrate on the filtering of one detector’s output, which is the first step in a detection process, the second one being the reconstruction of the gravitational wave signal from the filtered outputs of (at least) three detectors. The second step has been already studied in detail [31,32], while the first has attracted so far little attention in the literature. Here, we study three filtering ideas for the detection of bursts in the data of interferometric gravitational wave detectors, two of them being very general and the third one more specific. These methods are, namely, a “counting” method, where we count the number of bins which are larger than some threshold in a certain window, then a method based on the autocorrelation function of the detector data, and finally a filtering based on the correlation of the data with a peak generic function. For each of them, we develop the statistical properties of a link to Gaussian statistics, number of false alarms, threshold definition, etc. In order to quantify the performances of such filters, we use as gravitational wave signals the SN catalog from Zwerger and Müller available on the web [33], and compute, as a benchmark, for each of them, the maximal distance of detection obtained by the three filters; as a reference, we compare to the maximal detection distance calculated by optimal filtering. For this purpose, we will use, as a model for the detector noise, the minimum of the VIRGO sensitivity, which occurs precisely in the range of frequencies of interest.

Of course, any burst filtering is unable to distinguish a nonstationary noise from a real gravitational wave event: such filterings will be sensitive to transient noise as well as to gravitational bursts. The goal of burst filtering in one detector is then mainly to act as a trigger and select interesting data streams in order to investigate coincidences with other detectors. It will also be useful to identify and study nonstationary noise in a single interferometric detector, ultimately providing vetos or cleaning procedures for “known” nonstationary noise sources.

Finally, it is stressed that a general filtering approach, such as one of those proposed below, will be sensitive to unexpected sources and therefore may provide some insight into new physics.

II. BURST FILTERING: SOME IDEAS

Since we know little about the expected waveforms of burst gravitational wave sources, a robust filtering is required. Since we wish such a filtering to work as an on-line trigger, it should be fast. We study three of such filters in the following. Throughout the paper, we assume that the detector noise is white, stationary, and Gaussian with zero mean. For the numerical estimates, we chose the flat (amplitude) spectral density to be $h_n \approx 4 \times 10^{-23} / \sqrt{\text{Hz}}$ and the sampling frequency $f_s \approx 20$ kHz; so the standard deviation of the

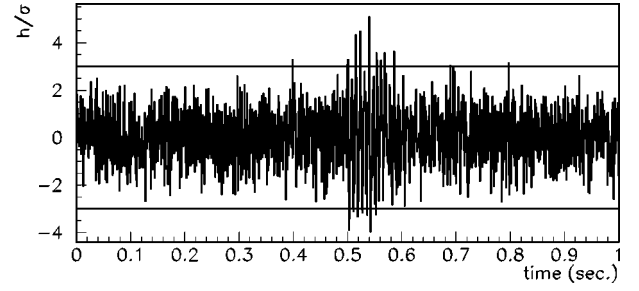


FIG. 1. Principle of the bin counting filter. The filter selects all bins that are above some level ($3\sigma_n$ in the example); here a signal, starting at time 0.5 s, has been superposed onto the noise.

noise is $\sigma_n = h_n \sqrt{f_s} \sim 6 \times 10^{-21}$. We will denote the sampling time $t_s = 1/f_s$. The value chosen for h_n corresponds approximately to the minimum of the sensitivity curve of the VIRGO detector [34]; around this minimum, the sensitivity is rather flat, in the range $\sim [200 \text{ Hz}, 1 \text{ kHz}]$, which is precisely the range of interest for the gravitational wave bursts we are interested in. This validates then our assumption of a white noise; otherwise, we can always assume that the detector output has been first whitened by a suitable filter [35].

A. Bin counting (BC)

The principle of this first filtering method is quite simple. A data stream of length T being given (so containing $N = T \times f_s$ data), we count the number of data (bins) whose value exceeds a certain threshold, say, $s \times \sigma_n$, in units of the noise standard deviation. The method is illustrated in Fig. 1. It follows the prescription about no preconceived idea about the waveforms to detect. In the absence of signal, the noise being Gaussian, the probability that a data bin x_i is larger than $s \times \sigma_n$ is

$$P(|x_i| \geq s \sigma_n) = 2 \int_s^\infty \frac{e^{-x^2/2}}{\sqrt{2\pi}} dx. \quad (2.1)$$

It is then straightforward that N_c , the number of bins above threshold, follows a binomial distribution and the probability that $N_c = n$ is

$$P(N_c = n) = \binom{N}{n} \left[\text{erfc} \left(\frac{s}{\sqrt{2}} \right) \right]^n \left[1 - \text{erfc} \left(\frac{s}{\sqrt{2}} \right) \right]^{N-n}, \quad (2.2)$$

where erfc is the complementary error function. Setting $p = \text{erfc}(s/\sqrt{2})$, the mean of N_c is then $\mu_c = Np$ and its standard deviation is $\sigma_c = \sqrt{Np(1-p)}$. It is well known that the normalized random variable $\tilde{N}_c = (N_c - \mu_c)/\sigma_c$ behaves like a normalized Gaussian variable, as soon as $Np > 5$ and $N(1-p) > 5$ [36]. These conditions will be satisfied in every situation of interest; so we will consider now that the random variable \tilde{N}_c is well approximated by a standard normal one.

Two parameters are involved in this method: the window length T (or equivalently N) and the threshold s . We will discuss the window length later, with the other filtering

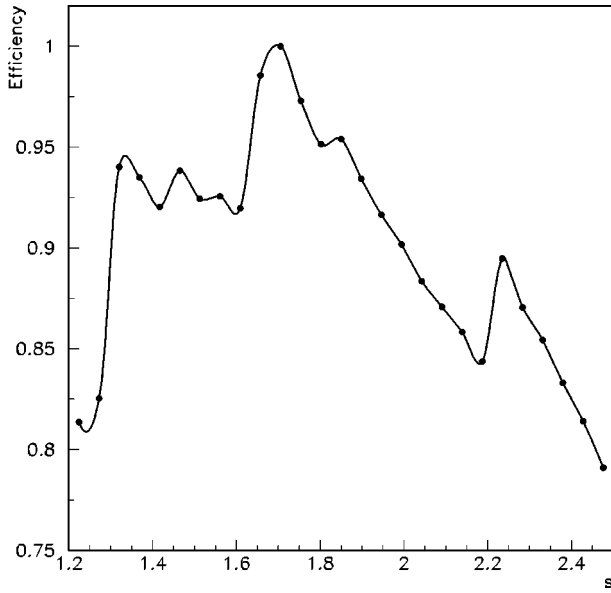


FIG. 2. Efficiency of the BC filter as a function of the threshold level s . The efficiency values have been normalized to the maximum value.

methods. On the contrary, the choice of s is a specific issue for this approach. First, s should not be too large, as we expect low amplitude signals. Then, s should not be too small because then the filter would become very sensitive to noise fluctuations with the drawback of a huge number of false alarms; as an example, if $s=2$, $P(|x_i| \geq 2\sigma_n) \approx 4.6\%$, giving on average 46 “counts” in a window of $N=1000$ sampled data. The optimal value for s is evaluated as follows: we compute the average distance of detection for the supernova signals of the Zwerger-Müller catalog as a function of s ; the calculation of this distance is explained with full details in Sec. III. Of course, many realizations of the noise are generated and the results are averaged in order to reduce the influence of noise fluctuations. The result can be seen in Fig. 2. We choose accordingly $s \approx 1.7$ in all the following, but any value of s in the range $[1.4, 2.0]$ would also be reasonable (giving a loss up to 10% in the average distance of detection with respect to the maximum).

B. Norm filter (NF)

This method has been initiated by the remark that white noise samplings are uncorrelated, while this is in general not true for a gravitational wave signal. So the autocorrelation $A_x(\tau) = \int x(t)x(t+\tau)dt$ of the detector output $x(t)$ should reveal the presence of a correlated signal hidden in a uncorrelated noise. However, two problems arise: the computing time (depending on the window length) and the choice of the detection criterion. The norm of the autocorrelation function seems a good one, since it should probably distinguish between noise and noise plus signal. But the squared norm of the autocorrelation of a Gaussian discrete variable is generally not a Gaussian variable itself: it becomes Gaussian only for very long data windows, as we have checked, and so it requires prohibitive calculation times. We could live with non-

Gaussian statistics, however, but we first require simplicity for these preliminary studies. This is why we turn our attention to the maximum of the autocorrelation, which is nothing but the squared norm of the output $x(t)$, since the autocorrelation of any function is maximal at zero. For the N sampled data in a window of size $T=N/f_s$, the output of this filter is then

$$A = \sum_{i=1}^{i=N} x(i)^2, \quad (2.3)$$

where $x(i)$ is the i th data in the window. When no signal is present, $x(i)$ is pure noise and, under our assumption of Gaussian noise, $x(i)^2$, being the square of a Gaussian random variable, is a chi-square random variable with one degree of freedom. A is then the sum of N such chi-square random variables with one degree of freedom, which is a chi-square random variable with N degrees of freedom. Its mean is $\mu_A = N$ and its standard deviation is $\sigma_A = \sqrt{2N}$. If $N > 30$, the random variable (related to the norm of the windowed detector output)

$$\tilde{A} = \sqrt{2A} - \sqrt{2N-1} \quad (2.4)$$

is very well approximated by a standard normal variable [36]. This fits the simplicity requirement and we will then use the output of \tilde{A} as a filter. The only parameter for this filter is the window size N ; it will be discussed in the next section.

C. Correlation with single pulses (PC)

Since many of the expected waveforms present one or several peaks, it seems judicious to use single pulses as filters. These pulses are modeled with truncated Gaussian functions such as

$$f_\tau(t) = \exp\left(-\frac{t^2}{2\tau^2}\right), \quad (2.5)$$

with t lying in the range $[-3\tau, +3\tau]$, so that the function is truncated at about 1% of its maximum value. The only parameter for this set of pulse filters is the width τ . The discrete correlation between the data $x(i)$, $i=1, \dots, N$, and the pulse can be written as

$$P(N, k) = \sum_{i=1}^N x(i+k) f_\tau([i-N/2]t_s). \quad (2.6)$$

In the absence of a signal, the output of the filter $P(N, k)$ is a Gaussian random variable, as a sum of Gaussian random variables weighted by the pulse function. The standard deviation of P is simply the square root of the sum of the squared weights,

$$\sigma_P = \sqrt{\sum_i f_\tau([i-N/2]t_s)^2}, \quad (2.7)$$

which can be recast as

$$\sigma_P^2 \approx \frac{1}{t_s} \int_{-Nt_s}^{Nt_s} f_\tau(t)^2 dt \approx \sqrt{\pi} \frac{\tau}{t_s}. \quad (2.8)$$

We can then define a signal to noise ratio (SNR) as the filter output normalized by the standard deviation σ_P : $\tilde{P} = P/\sigma_P$, where P is the maximum of the function defined in Eq. (2.6).

D. Practical implementation

The two first methods BC and NF are very easy to implement in practice, as we can write simple recurrence relations for the calculation of the filter outputs in a given window, as a function of the filter outputs in the previous window. For instance, for the BC, the output of the filter in a window of length N starting at the m th datum $x(m)$ and ending at the datum $x(m+N-1)$ is $N_c(m)$. The next filter output $N_c(m+1)$ is obtained by moving the window by one bin, namely, starting now at the datum $x(m+1)$ and ending at the datum $x(m+N)$. The relation between $N_c(m)$ and $N_c(m+1)$ can be cast as

$$N_c(m+1) = N_c(m) + \Theta(m+1) - \Theta(m), \quad (2.9)$$

where $\Theta(i) = 1$ if the datum $x(i)$ is above threshold $s \times \sigma_n$ and $\Theta(i) = 0$ if $x(i)$ is below.

Similarly, for the NF, in the window of length N starting at the datum $x(m+1)$, the norm of the data is $A(m+1) = \sum_{i=m+1}^{m+N} x(i)^2$ and is simply related to $A(m)$ by $A(m+1) = A(m) + x(m+N)^2 - x(m)^2$. This recurrence relation between $A(m+1)$ and $A(m)$ allows a very fast calculation of the filter output $\tilde{A}(m+1)$ to be performed from the calculation of the previous filter output $\tilde{A}(m)$.

One advantage of this practical simplicity for both methods is that it allows the computation of filter outputs with a window moving from bin to bin, which is not always possible (and anyway not necessary) in case of correlations with a predefined lattice of filters.

Concerning the PC, we have first to build the lattice of filter, depending on only one parameter, the Gaussian peak standard deviation τ . The parameter space is the interval $[\tau_{\min}, \tau_{\max}]$. The distance between two successive filters of the lattice is denoted $\Delta\tau$ and the problem is to estimate $\Delta\tau$, which is *a priori* a function of τ . The output of the correlation between a Gaussian peak filter f_τ and a ‘‘signal’’ g is

$$\langle f_\tau, g \rangle = K \operatorname{Max}_{t'} \frac{\int f_\tau(t+t')g(t)dt}{\sqrt{\int f_\tau^2(t)dt}}, \quad (2.10)$$

where K is a constant. If g is itself a filter of the kind f'_τ , it is easy to show that the maximal correlation is obtained for $t' = 0$. Following [37], we chose $\Delta\tau$ such that

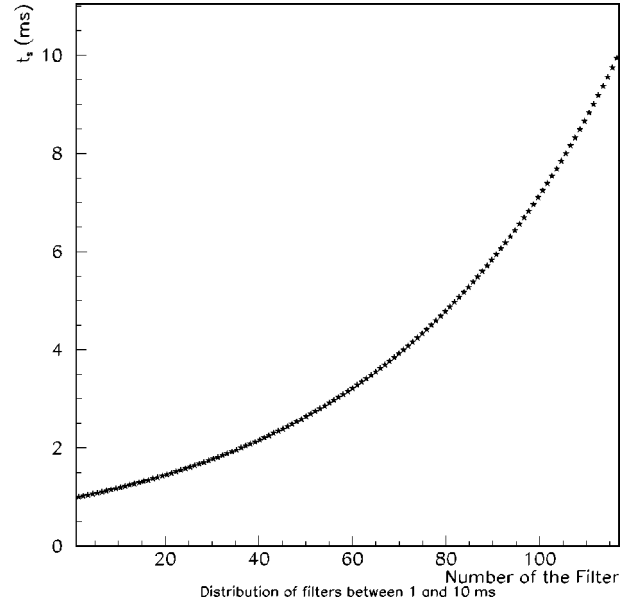


FIG. 3. Distribution of the 117 templates for the peak correlator in the interval $[1;10]$ ms with the assumption $\epsilon = 10^{-4}$.

$$\frac{\langle f_\tau, f_\tau \rangle - \langle f_{\tau+\Delta\tau}, f_\tau \rangle}{\langle f_\tau, f_\tau \rangle} \leq \epsilon, \quad (2.11)$$

where ϵ is the allowed loss in the signal to noise ratio. Expanding the ratio of Eq. (2.11) to second order in $\Delta\tau/\tau$ leads to the simple inequality

$$\left(\frac{\Delta\tau}{\tau}\right)^2 \leq 4\epsilon. \quad (2.12)$$

If the Gaussian filter f_τ of width τ belongs to the lattice, then the next one $f_{\tau+\Delta\tau}$ is built from

$$\Delta\tau = 2\tau\sqrt{\epsilon}. \quad (2.13)$$

Starting from the first filter of width τ_{\min} , it is then easy to build the k th filter: its width is $\tau_k = (1 + 2\sqrt{\epsilon})^{k-1} \tau_{\min}$. The total number of templates in the lattice is finally the maximal integer n_t such that $(1 + 2\sqrt{\epsilon})^{n_t-1} \tau_{\min} \leq \tau_{\max}$.

For example, Fig. 3 shows the distribution of the 117 templates in the interval $[1 \text{ ms}, 10 \text{ ms}]$ for a loss in SNR of $\epsilon = 10^{-4}$ (the one we will use in the next section); the choice of $\epsilon = 10^{-2}$ reduces the number of filters to 13 for the same interval. We notice that we can allow for a very low loss in SNR and still obtain a reasonable number of templates; this is due both to the fact that we deal with one-dimensional lattice space and to the ‘‘smooth’’ dependence of n_t on ϵ . For instance, the same very low value of $\epsilon = 10^{-4}$ and a parameter space extended to the (physically possible) interval $[1 \text{ ms}, 1 \text{ s}]$ lead to a lattice of only 349 templates, which is easy to implement for an on-line processing.

E. Threshold and false alarms

Since the outputs of the three proposed filters behave like standard normal random variables (when no signal is

present), it is convenient to define the same detection threshold for all, with, consequently, the same number of false alarms produced. As we expect weak signals, this threshold has to be low. On the other hand, we can deal with a large number of false alarms; these spurious events can be processed and discarded later when working in coincidence with other detectors. The relation between the detection threshold η and the rate of false alarms r_{fa} for a Gaussian random variable is

$$2 \times \frac{1}{\sqrt{2\pi}} \int_{\eta}^{\infty} \exp\left(-\frac{x^2}{2}\right) dx = r_{fa}. \quad (2.14)$$

A false alarm rate $r_{fa} = 5 \times 10^{-7}$ (≈ 36 false alarms per hour for a sampling rate $f_s = 20$ kHz) corresponds to a threshold $\eta \approx 4.75$, while a false alarm rate 10 times smaller corresponds to $\eta \approx 5.20$. For the results presented in the following), the chosen threshold is $\eta \approx 4.75$.

For the two first filtering methods, BC and NF, the situation is, however, not so simple because the outputs of the filters in two successive windows are in fact strongly correlated. For example, for the BC filtering, the filter outputs in two successive windows [starting, respectively, at the data $x(m)$ and $x(m+1)$] are related by Eq. (2.9); it is clear that $N_c(m)$ and $N_c(m+1)$ are the same or differ at most by ± 1 . So if the detection threshold is exceeded in a number of consecutive windows, there is in general only one ‘‘event.’’ This leads us to redefine what is a detected event: an event is said to be detected in some time interval $[m_1 t_s, m_2 t_s]$ if the filter output $O(m)$ exceeds the threshold η for all values of m in the interval $[m_1, m_2]$ and is less than η outside. This is equivalent to defining a ‘‘correlation length’’ $(m_2 - m_1) t_s$ for the event to be detected.

III. DETECTION OF SUPERNOVAS

In this section, we use the catalog of simulated gravitational wave signals emitted during supernova collapses and computed by Zwerger and Müller [20], to implement and test the three filterings described previously, in a realistic context.

A. Catalog

The catalog of Zwerger and Müller [33] contains 78 gravitational wave signals generated by axisymmetric core collapses. Note that, in particular due to axisymmetry, these are purely linearly polarized waves ($h_{\times} = 0$). Each of them corresponds to a particular set of parameters, essentially the initial distribution of angular momentum and the rotational energy of the star core, in the collapse models of Zwerger and Müller. The signal total durations range from about 40 ms to a little more than 200 ms. The gravitational wave amplitudes of the stronger signals are of the order $h(=h_+) \sim$ a few 10^{-23} for a source located at 10 Mpc; that leaves little hope to detect such events with the first generation detectors. Concerning the shape of the waveforms (see Fig. 4), Zwerger and Müller distinguish three different types of

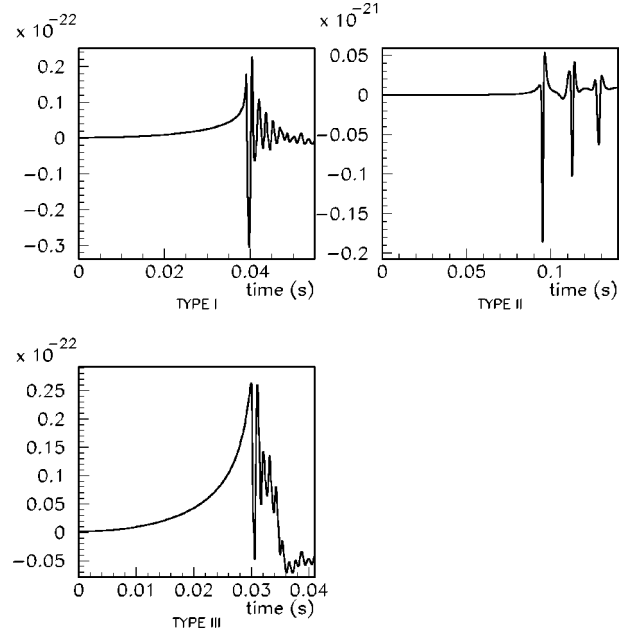


FIG. 4. Typical waveforms for the type I, II, and III supernova signals in the Zwerger-Müller catalog.

signals [20]. Type I signals typically present a first peak (associated with the bounce) followed by a ringdown. Type II signals show a few (two to three) decreasing peaks, with a time lag between the first two of at least 10 ms. Type III signals exhibit no strong peak but fast (~ 1 kHz) oscillations after the bounce. The fact that type I and type II signals are characterized by strong peaks validates the choice of filtering by correlation with generic peaks in order to detect such events. The 78 signal templates in the catalog are not equally sampled; so we have first resampled them by interpolation at the desired sampling frequency ($f_s = 20$ kHz in our examples).

B. Optimal filtering and maximal distances of detection

Since the 78 signal waveforms are known, we can explicitly derive the optimal SNR provided by the Wiener filter for each of them, and then compute the maximal distance of detection. We will then be able to build a benchmark for the different filters by comparing their results (detection distances) to the results of the Wiener filter. In all the following, we assume that the incoming waves have an optimal incidence with respect to the interferometric detector.

Let us call $h(t)$ one of the 78 signals and $\tilde{h}(f)$ its Fourier transform. The optimal signal to noise ratio ρ_0 is given by

$$\rho_0^2 = 2 \int \frac{|\tilde{h}(f)|^2}{S_h(f)} df, \quad (3.1)$$

where S_h is the one-sided noise power spectral density (hence the factor of 2). The noise is assumed to be Gaussian and white with a standard deviation related to the constant spectral density $S_h = h_n^2$ by $\sigma_n = h_n \times \sqrt{f_s} = \sqrt{S_h \times f_s}$. The SNR then becomes

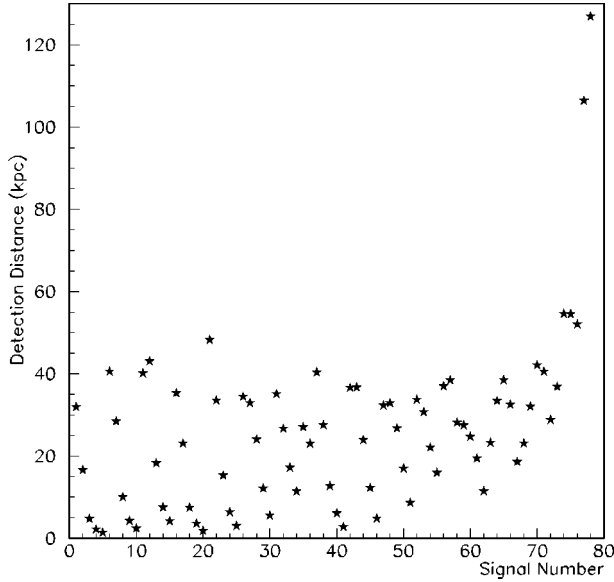


FIG. 5. Detection distances calculated with the optimal filter for the 78 signals in the catalog of Zwerger and Müller. About 6 signals can be detected at distances as high as about 50 kpc (the LMC distance).

$$\rho_0^2 = \frac{2f_s}{\sigma_n^2} \int |\tilde{h}(f)|^2 df = \frac{2f_s}{\sigma_n^2} \int |h(t)|^2 dt. \quad (3.2)$$

As previously, a supernova signal is detected by the Wiener filter if $\rho_0 \geq \eta$, where η is the same detection threshold as defined above. Figure 5 shows the maximal distance of detection for each of the 78 signals. The mean distance, averaged over all the signals, is about 26.1 kpc, which is of the order of the diameter of the Milky Way. A few signals can be detected at distances beyond 50 kpc, the distance of the Large Magellanic Cloud (LMC). The most energetic signals (Nos. 77 and 78) can be detected at distances as high as 100–120 kpc. It is clear that this class of signals will be detected by the first generation interferometric detectors only if the supernovas occur inside our Galaxy or in the very close neighborhood.

C. Detection by the three filters

1. Window sizing

The window size N for the first two filters is a compromise between the need for not too small number of bins, in order to guarantee that the filter outputs are well approximated by Gaussian random variables and the rather short signals we are looking for. The first constraint is easily satisfied for the NF method, where N must be larger than about 30. For the BC method, we must have $N \text{erfc}(s/\sqrt{2}) > 5$ and $N[1 - \text{erfc}(s/\sqrt{2})] > 5$; with the optimal choice of $s = 1.7$, so that $\text{erfc}(s/\sqrt{2}) \approx 0.91$, the two inequalities give, respectively, $N > 6$ and $N > 56$. The constraints are not very severe and require that N must be between 80 and 150, as has been checked by Monte Carlo simulations (looking for the optimal window size giving the maximal mean distance of detection).

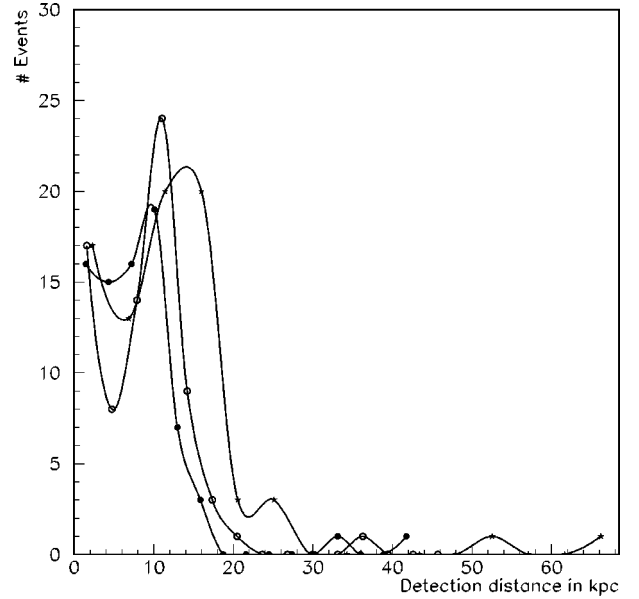


FIG. 6. Histogram of the number of signals as a function of the maximal detection distance for each of the three filters (●, BC; ○, NF, and ★: PC).

For the pulse filter PC, the window size is automatically fixed by the definition interval of the Gaussian peak $[-3\tau, 3\tau]$ for a filter of width τ . The window size for the correlation with the filter f_τ is then $N = 6\tau f_s$ and depends on τ .

2. Detection distance

The efficiency of each filter is measured by the maximal distance of detection for each of the 78 gravitational wave signals of the catalog. This distance is obtained by averaging over many noise realizations in a Monte Carlo simulation. We present the results in two ways. Figure 6 shows the number of detected signals as a function of the distance of detection for the three filters. The results of Fig. 6 combined with the results for the optimal filtering (Fig. 5) are reported in Fig. 7 in a normalized way. The histograms in Fig. 7 show the number of signals detected as a function of the reduced distance of detection for the three filters; the reduced distance of detection is simply the distance of detection divided by the maximal distance of detection computed with the optimal filter. The means of the distributions are, respectively, 0.22, 0.26, and 0.34 for the BC, NF, and PC filters; these can be seen as rough estimators of the efficiency of the filters. The histograms in Fig. 7 give also an idea of the sensitivity of the filters to the waveforms of the detected signals. We note that the histograms corresponding to the BC and NF filters are much more concentrated than the one corresponding to the PC filter; this is particularly impressive for the NF filter. This means that the two first filters are rather robust and their efficiency does not crucially depend on the details of the gravitational wave signals. On the contrary, the larger dispersion of the last histogram (PC) indicates that the response of the PC filter depends much more on the gravitational waveform.

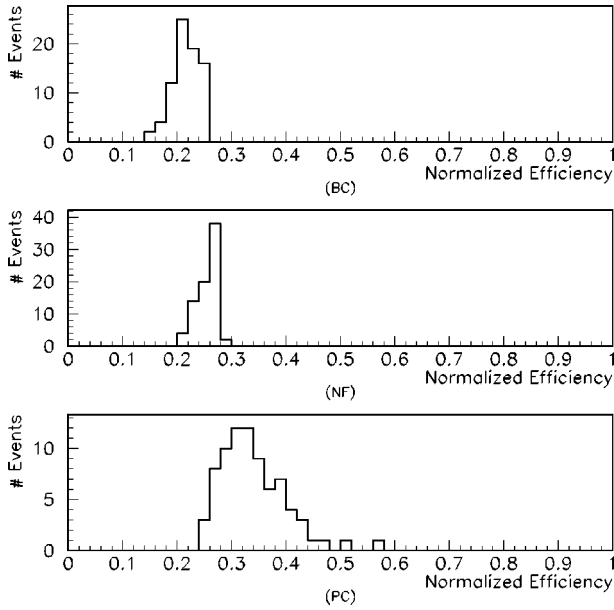


FIG. 7. Histogram of the number of signals as a function of the normalized detection distance for each of the three filters. The normalized distance is the detection distance divided by the corresponding maximal detection distance computed by the optimal filtering.

The global efficiency can be measured as the mean detection distance averaged over the 78 signals. The results are reported in Table I. The efficiency of the BC and NF filters is about one-third of the efficiency of the optimal filtering (maximum efficiency), while the PC filter (for $\epsilon = 10^{-4}$) has an efficiency about 58% of the maximal efficiency.

We note that none of the BC, NF, and PC filters is efficient enough to cover all the Galaxy on average. Several signals, however can be “seen” anywhere from the Galaxy and even beyond; in particular the signals 77 and 78 can be detected up to the LMC by any of the three filters.

In fact, concerning the PC filter, the mean distance of detection depends on ϵ , the allowed loss in SNR, and consequently on the number of filters in the lattice. Figure 8 shows the mean distance of detection as a function of the loss in SNR. As ϵ decreases, the mean distance of detection becomes closer to the maximal value (a little larger than 15 kpc). We also notice that for high values of ϵ (low number of templates), for instance, above $\epsilon = 1\%$ (13 templates), the efficiency of the PC filter is still well larger than the NF/BC efficiency.

3. Computation time considerations

Apart from the criterion of simplicity of the filters, we require also that the data processing with these filters has to be fast enough to be implemented on-line as a trigger.

TABLE I. Detection distance averaged over the 78 signals for the different filters.

Filter	Optimal	BC	NF	PC
Average distance (kpc)	26.1	7.8	9.3	15.2

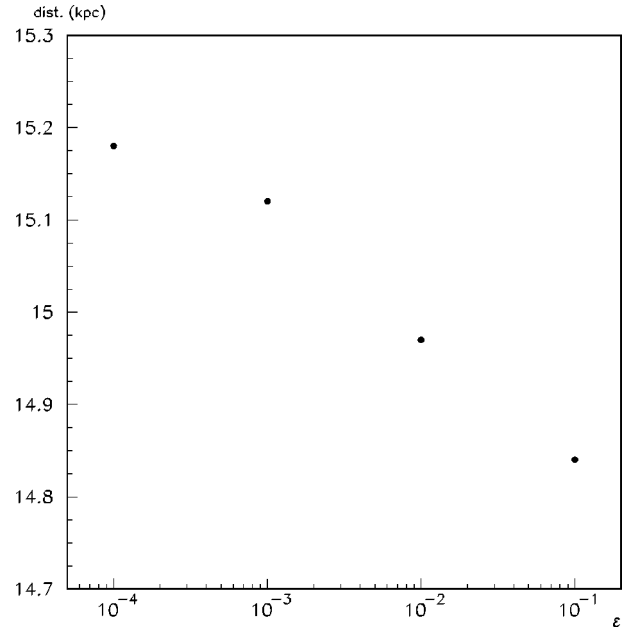


FIG. 8. Efficiency of the peak correlator PC versus the loss in SNR ϵ . The efficiency is measured as the mean detection distance for the 78 signals in the Zwinger-Müller catalog.

An analysis of one day of data has been performed (in order to check the validity of the redefinition of an event—see Sec. II E—and the number of false alarms) on a DEC Alpha workstation, in about 14 mn with the BC filtering and in about 25 mn with the NF filtering. So there is about a factor 100 (57) between the data stream duration and the time needed to process them by the BC filter (the NF filter). These two filters can then be used on-line without any problem.

The PC filter is no more problematic due to implementation in the Fourier space and use of fast Fourier transformations (FFT's). Moreover, the correlations do not need to be computed in successive windows. Indeed a template f_s (Gaussian of width s) has a certain correlation length ($\sqrt{2}s$); so it is possible to compute the correlation with the template f_s every T_s , where T_s is related to the allowed loss in filter efficiency. In practice, one order of magnitude in the calculation time can be gained with a loss of 1–2 % of efficiency.

IV. CONCLUSION

We have studied in this paper three filtering methods with the aim of building on-line triggers for the selection of burst-like events in the data flow of interferometric gravitational wave detectors. Such a filtering needs first to be as general and as simple as possible; these two prescriptions are satisfied well by the two first: BC and NF filterings. A third filter has then been studied in order to quantify what could be the gain with a more specific filtering, i.e., using some *a priori* information on the signals to detect (namely, here the fact that the supernova signals contain at least one peak of short duration). The catalog of supernova gravitational wave signals provided by Zwinger and Müller has been used in order to build a benchmark for the different filters in a realistic

way and to compare each of them to the optimal (Wiener) filter.

The results we find are first that a general filter, such as BC or NF, has an efficiency of about one-third (0.30–0.36) of the efficiency of the optimal filter (maximal efficiency for a linear filter). The peak correlator PC (looking for the peaks in the Zwerger-Müller signals) has an efficiency slightly larger (58% of the optimal filter efficiency). We note also that the general filters seem to be more robust (less sensitive to the waveform details) than the peak correlator, because of the smaller dispersion of their (normalized) responses to the 78 supernova signals.

Concerning a practical implementation, each of the filters can be implemented on line and can be used as a trigger in order to select events for off-line coincidences with other detectors.

The results for the detection of the Zwerger-Müller signals are not very optimistic. Moreover, as we have assumed optimal incidence for the gravitational waves, the detection distances should be divided by $\sqrt{5}$ for sources randomly dis-

tributed over the sky [5]. So only a small fraction of the supernova events can be detected anywhere in the Galaxy or beyond. This is not a surprise and, anyway, not the main point of this paper.

We finally notice that the two general burst filters BC and NF we studied are in fact nonlinear filters (they cannot be reduced to a correlation with the detector output). This may encourage physicists to develop and study such a class of filters in the context of gravitational wave detection. In the near future, we plan to study other filters based on the auto-correlation function and on wavelet analysis. We plan also to study the effect of a more realistic noise on the response of this class of filters, in particular the effect of non-Gaussianity and nonstationarity. We keep in mind that nonstationary noises can be treated as “signals” and the burst filtering can help to identify them and finally understand the detector behavior.

Note added in proof. A filter similar to our Norm Filter (NF) has been proposed by Flanagan and Hughes in the context of the detection of black hole mergers [38].

-
- [1] A. Abramovici, W.E. Althouse, R.W.P. Drever, Y. Gürsel, S. Kawamura, F.J. Raab, D. Shoemaker, L. Sievers, R.E. Spero, K.S. Thorne, R.E. Vogt, R. Weiss, S.E. Whitcomb, and M.E. Zucker, *Science* **256**, 325 (1992).
 - [2] B. Caron *et al.* *Nucl. Phys. B (Proc. Suppl.)* **54B**, 167 (1997).
 - [3] K. Danzmann *et al.*, in *Gravitational Wave Experiments*, edited by E. Coccia, G. Pizzella, and F. Ronga (World Scientific, Singapore, 1995).
 - [4] K. Kuroda, in *Gravitational Waves: Sources and Detectors*, edited by I. Ciufolini and F. Fidicaro (World Scientific, Singapore, 1997).
 - [5] K.S. Thorne, in *300 Years of Gravitation*, edited by S.W. Hawking and W. Israel (Cambridge University Press, Cambridge, England, 1987).
 - [6] S. Bonazzola and J.-A. Marck, *Annu. Rev. Nucl. Part. Sci.* **45**, 655 (1994).
 - [7] B.F. Schutz, in *The Detection of Gravitational Waves*, edited by D.G. Blair (Cambridge University Press, Cambridge, England, 1991).
 - [8] S.V. Dhurandhar and B.F. Schutz, *Phys. Rev. D* **50**, 2390 (1994).
 - [9] T.A. Apostolatos, *Phys. Rev. D* **54**, 2421 (1996).
 - [10] B.S. Sathyaprakash, in *Relativistic Gravitation and Gravitational Waves*, edited by J.-A. Marck and J.-P. Lasota (Cambridge University Press, Cambridge, England, 1997).
 - [11] A. Królak and P. Trzaskoma, *Class. Quantum Grav.* **13**, 813 (1996).
 - [12] J.-M. Innocent and B. Torr sani, in *Mathematics of Gravitation*, edited by A. Królak (Banach Center Publications, Warsaw, 1997).
 - [13] L.S. Finn and D.F. Chernoff, *Phys. Rev. D* **47**, 2198 (1993).
 - [14] R. Balasubramanian and S.V. Dhurandhar, *Phys. Rev. D* **57**, 3408 (1998).
 - [15] D. Nicholson and A. Vecchio, *Phys. Rev. D* **57**, 4588 (1998).
 - [16] P.R. Brady, T. Creighton, C. Cutler, and B.F. Schutz, *Phys. Rev. D* **57**, 2101 (1998).
 - [17] L.S. Finn and C.R. Evans, *Astrophys. J.* **351**, 588 (1990).
 - [18] R. M nchmeyer, G. Sch fer, E. M ller, and R.E. Kates, *Astron. Astrophys.* **246**, 417 (1991).
 - [19] S. Bonazzola and J.-A. Marck, *Astron. Astrophys.* **267**, 623 (1993).
 - [20] T. Zwerger and E. M ller, *Astron. Astrophys.* **320**, 209 (1997).
 - [21] M. Rampp, E. M ller, and M. Ruffert, *Astron. Astrophys.* **332**, 969 (1998).
 - [22] J.M. Cordes, R.W. Romani, and S.C. Lundgren, *Nature (London)* **362**, 133 (1993).
 - [23] S.N. Nazin and K.A. Postnov, *Astron. Astrophys.* **317**, L79 (1997).
 - [24] R.F. Stark and T. Piran, *Phys. Rev. Lett.* **55**, 891 (1985).
 - [25] L. Blanchet, in *Proceedings of the Second Workshop on Gravitational Wave Data Analysis*, edited by M. Davier and P. Hello (Editions Fronti res, Paris, 1998).
 - [26] K. Oohara and T. Nakamura, in *Relativistic Gravitation and Gravitational Waves*, edited by J.-A. Marck and J.-P. Lasota (Cambridge University Press, Cambridge, England, 1997).
 - [27] M. Ruffert and H.-Th. Janka, *Astron. Astrophys.* **338**, 535 (1998).
 - [28] L.S. Finn, in *Proceedings of the 14th International Conference on General Relativity and Gravitation*, edited by M. Francaviglia, G. Longhi, L. Lusanna, and E. Sorace (World Scientific, Singapore, 1997). See also the Binary Black Hole Grand Challenge Alliance web page at <http://www.npac.syr.edu/projects/bh/>.
 - [29] S. Detweiler, *Astrophys. J.* **239**, 292 (1980).
 - [30] F. Echeverria, *Phys. Rev. D* **40**, 3194 (1989).
 - [31] S. V. Dhurandhar and M. Tinto, *Mon. Not. R. Astron. Soc.* **234**, 663 (1988).

- [32] Y. Gürsel and M. Tinto, *Phys. Rev. D* **40**, 3884 (1989).
- [33] <http://www.mpa-garching.mpg.de/~ewald/GRAV/grav.html>.
- [34] The “official” VIRGO sensitivity curve is available at : <http://www.pg.infn.it/virgo/presentation.htm>.
- [35] M. Beccaria, E. Cuoco, and G. Curci, “Adaptive Identification of VIRGO-like noise spectrum,” internal VIRGO Report No. VIR-NOT-PIS-1390-096, 1997. See also M. Beccaria, E. Cuoco, and G. Curci, in Proceedings of the Second Edoardo Amaldi Conference on Gravitational Waves, Geneva, Switzerland, 1997.
- [36] M.R. Spiegel, *Probabilités et Statistique, Cours et Problèmes* (McGraw-Hill, Paris, 1981).
- [37] B.S. Sathyaprakash and S.V. Dhurandhar, *Phys. Rev. D* **44**, 3819 (1991).
- [38] E. E. Flanagan and S. A. Hughes, *Phys. Rev. D* **57**, 4535 (1998).